Spectral Super-Resolution for Hyperspectral Images via Sparse Representations

Konstantina Fotiadou, Grigorios Tsagkatakis and Panagiotis Tsakalides

Abstract— **The spectral dimension of hyperspectral imaging (HSI) systems plays a fundamental role in numerous terrestrial and earth observation applications, including spectral unmixing, target detection, and classification among others. However, in several cases the spectral resolution of HSI systems is sacrificed for the shake of spatial resolution, as such in the case of snapshot spectral imaging systems that acquire simultaneously the 3D data-cube. We address these limitations by introducing an efficient post-acquisition spectral resolution enhancement scheme that synthesizes the full spectrum from only few acquired spectral bands. To achieve this goal we utilize a regularized sparse-based learning procedure where the relations between high and low-spectral resolution hyper-pixels are efficiently encoded via a coupled dictionary learning scheme. Experimental results and quantitative validation on data acquired by NASA's EO-1 mission's Hyperion sensor, demonstrate the potential of the proposed approach for accurate spectral resolution enhancement of hyperspectral imaging systems.**

I. INTRODUCTION

Over the last decades Hyperspectral Imaging (HSI) systems created an enormous outburst in the field of earth observation. Multiple instrument on-board imaging systems are currently available, providing a large amount of hyperspectral imagery for various applications, such as precision agriculture, geology and oceanography. Despite the important advantages hyperspectral imaging systems demonstrate, HSI acquisition and processing stages usually introduce multiple constraints. Slow acquisition time, limited spectral and spatial resolution, low dynamic range, and restricted field of view, are just a few of the limitations that hyperspectral sensors admit, and require further investigation.

K. Fotiadou is with the Department of Computer Science, University of Crete, Greece and the Institute of Computer Science - F.O.R.T.H., Crete, Greece. E-mail: kfot@ics.forth.gr

G. Tsagkatakis is with the Institute of Computer Science - F.O.R.T.H. E-mail: greg@ics.forth.gr

P. Tsakalides is with the Department of Computer Science, University of Crete, Greece and the Institute of Computer Science - F.O.R.T.H., Crete, Greece,E-mail: tsakalid@ics.forth.gr

Enhancing the spectral quality of the acquired hyperspectral scenes is critical for both visualization and subsequent analysis, including spectral unmixing, pixel classification and region clustering. Additionally, high-spectral resolution imaging systems are able to capture and process a huge amount of data, including the 2D spatial and the 1D spectral variations of an input scene over time. Unfortunately, various factors can lead to the introduction of imaging constraints such as the case of Snapshot Spectral Imaging systems that directly acquire the entire 3D data-cube through a convenient combination of spectral filters and detector elements. Despite the dramatic reduction these systems exhibit with respect to acquisition time, they also reduce the spectral resolution, for example, by associating each pixel with a single spectral band in the Spectrally Resolvable Detector Arrays. Another limitation arises from remote sensing data, where for instance multi-spectral sensors such as MODIS resolve a limited number of spectral bands with a known revisit frequency, while tasked hyperspectral sensors such as NASA's EO-1 mission's Hyperion sensor, acquire a huge number of spectral bands with undefined revisit frequency. In remote sensing community, the main challenge is to combine high revisit frequency and high number of acquired spectral bands.

In order to overcome the aforementioned limitations, we propose a novel, post-acquisition spectral resolution enhancement technique that recovers the full-spectrum from a limited number of spectral observations, based on the state-of-the-art mathematical frameworks of Sparse Representations (SR) and joint dictionary learning (DL) [1]. Unlike state-of-the-art hyperspectral super-resolution methods that utilize inherent correlations to obtain high spatial resolution images, the proposed algorithm aims at enhancing the spectral content of the imagery. This goal is achieved by introducing the assumption that each high spectral resolution "hyper-pixel" is estimated from its low spectral resolution version, identifying a sparse representation encoding that directly generates the high-spectral resolution output.

The notion of sparsity has revolutionized modern signal processing and machine learning applications, and has lead to very impressive results in a variety of imaging processing and computer vision tasks, including image deblurring, super-resolution, denoising, classification etc. In this work, we enforce the sparsity constraint, learning a joint sparse coding dictionary from multiple correspondent low and high spectral resolution training pairs. To the best of our knowledge, only a handful of techniques have been proposed in literature that recover the full spectrum information of multi- and hyperspectral imagery, from a limited number of input, low spectral resolution bands. Specifically, in our previous work, [2] we addressed the problem of spectral resolution enhancement of hyperspectral imagery and we applied on hyperspectral data acquired by a Ximea camera equipped with IMEC's 5×5 snapshot mosaic hyperspectral sensors [3], [4]. These intelligent sensors multiplex optically the 3D spatio-spectral information on a two-dimensional CMOS detector array, where a layer of Faby-Perot spectral filters is deposited on top of the detector array. The hyperspectral data is initially acquired in the form of 2D mosaic images. In order to generate the 3D hypercubes, the spectral components are properly rearranged into separate spectral bands. In this work, we apply our proposed spectral super-resolution scheme on remote sensing hyperspectral data acquired by NASA's EO-1 Hyperion sensor.

The rest of this paper is structured as follows. Section II provides an overview of the related work concerning the spatial and spectral resolution enhancement of hyperspectral imaging systems. Section III presents the formulation of the spectral super-resolution scheme of and hyperspectral imagery considered in this work, whereas Section IV exposes our proposed solution. Section V reports the experimental results, while conclusions and extensions of this work are presented in Section VI.

II. Related Work

The majority of hyperspectral resolution enhancement approaches focus on the spatial resolution of HSI imagery. Current spatial resolution enhancement approaches may be discriminated into two characteristic categories: pan-sharpening and spatio-spectral fusion techniques. Pan-sharpening techniques [5] combine a low spatial resolution hyperspectral scene with the correspondent high spatial resolution panchromatic image to synthesize the high spatial 3D data cube. On the other hand, spatio-spectral fusion approaches improve the spatial resolution exploiting relations between the spatial and the spectral variations of HSI scenes. Specifically, the authors in [6] enhance the spatial dimension of HSI, by performing a sparse spectral unmixing technique and fusing the results with the multispectral imagery. Similarly, in [7] is formulated a joint super-resolution and unmixing approach, based on a sparse representation in the spatial domain, and a spectral unmixing in the spectral domain to achieve the enhancement. In contrast, in [8] the authors propose a spatial super-resolution technique, without using any additional image with higher spatial resolution. Specifically, they utilize a fully constrained least squares spectral unmixing scheme, with a spatial regularization based on modified binary particle swarm optimization. Besides fusion-based approaches, over the last years multiple techniques exploit the low-rank matrix completion and sparse representation frameworks to super-resolve low spatial resolution HSI scenes. Specifically, the authors in [9] propose a novel approach that estimates high spatial and spectral resolution hypercubes extending the traditional formulation of Matrix Completion by introducing non-negativity constraints during the recovery process.

In contrast to the spatial super-resolution, enhancing the spectral dimension of HSI scenes, has drawn little attention. On that note, the authors in [10] utilize a hardware solution to amplify the spectral dimension of HSI imagery. Specifically, they propose a generalization of the Coded Aperture Snapshot Spectral (CASSI) imaging system, by using a pair of high resolution coded apertures, able to encode both spatio-spectral dimensions of hyperspectral scenes. Another spectral resolution enhancement technique is demonstrated in [11], where the authors consider geographically co-located multispectral and hyperspectral oceanic water-color images and they enhance the limited multispectral measurements utilizing a sparsity based approach. First, they use a spectral mixing formulation and they define the measured spectrum for each pixel as the sum of the weighted material spectra. The desired high-spectral resolution spectra is expressed as a linear combination between a blurring matrix and the measured spectra, while this problem is solved via a sparse-based formulation.

III. Problem Formulation

This work proposes a novel scheme for synthesizing high-spectral resolution hyperspectral scenes from few acquired measurements. Formally, let $\mathbf{S}_\ell$ be the low-

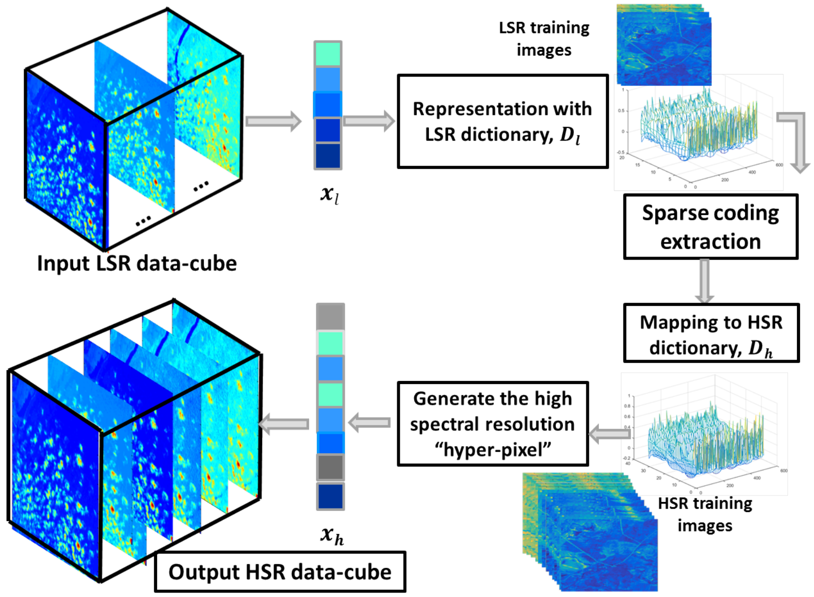

Fig. 1: Proposed Block Diagram: Our algorithm takes as input a hypercube acquired with a limited number of spectral bands and reconstructs the full spectrum of the scene.

spectral resolution 3D data-cube acquired with M spectral bands. Our task is to estimate the missing bands, in order to generate the full spectrum composed of N spectral bands.

A. Sparse Representations

The proposed approach synthesizes a high-spectral resolution data-cube from its acquired low-spectral resolution form, by capitalizing on the *Sparse Representations* (SR) framework [1], [12]. According to SR, features learnt from high or low spectral resolution "hyper-pixels" can be represented as sparse linear combinations of elements with respect to their over-complete dictionaries. Additionally, the theory of SR suggests that the same sparse coding $\mathbf{w} \in \mathbb{R}^N$ can be utilized among the two representations, provided that proper dictionary matrices are jointly learned.

Formally, each input low-spectral resolution "hyper-pixel" $\mathbf{s}_\ell \in \mathbb{R}^M$, can be expressed as a linear combinations between a sparse code vector $\mathbf{w} \in \mathbb{R}^N$, and a representation matrix, $\mathbf{D}_h \in \mathbb{R}^{M\times N}$, created by training low-spectral resolution hyper-pixels, according to:

$$\mathbf{s}_l = \mathbf{D}_l \mathbf{w}$$

IV. Proposed Solution

Recovery of the sparse code vector $\mathbf{w} \in \mathbb{R}^N$ is accomplished by solving the following minimization problem:

$$\min_{\mathbf{w}} ||\mathbf{w}||_0 \quad \text{subject to} \quad ||\mathbf{s}_\ell - \mathbf{D}_\ell \mathbf{w}||_2^2 < \epsilon, \qquad (1)$$

where ϵ denotes the approximation error modelling the noise properties, and $||\mathbf{w}||_0 = \#(i|\mathbf{w}_i \neq 0)$ stands for the ℓ_0 pseudo-norm. Despite the ℓ_0-norm is a convenient choice, it makes the optimization intractable. Fortunately, the ℓ_0-norm can be relaxed into a higher-order norm minimization problem, such as the convex ℓ_1-norm, $\ell_1 = \sum_i |\mathbf{w}_i|$, leading to robust solutions. Alternatively, the optimization problem is formulated as:

$$\min_{\mathbf{w}} ||\mathbf{s}_\ell - \mathbf{D}_\ell \mathbf{w}||_2^2 + \lambda ||\mathbf{w}||_1, \qquad (2)$$

where the parameter λ regularizes the fidely of the solution. The joint training of the low and high spectral resolution dictionaries, guarantees that approximately the same sparse coding can be utilized among the two representations. Proceeding to the decoding step, the optimal sparse code $\mathbf{w}^\star$ from Eq. 2, is directly projected onto the high-spectral resolution dictionary $\mathbf{D}_h$ to synthesize the high-spectral resolution "hyper-pixel", as

$$\mathbf{s}_h = \mathbf{D}_h \mathbf{w}^\star, \qquad (3)$$

The concatenation of all the recovered high-spectral resolution "hyper-pixels", synthesizes the high-spectral resolution 3D data-cube. The main objective of this work arises from the proper learning of the dictionary matrices $\mathbf{D}_\ell$, and $\mathbf{D}_h$ in order to sparsify both the low and the higher spectral resolution data. The following subsection discusses thoroughly the proposed dictionary learning scheme.

A. *Joint Dictionary Learning*

Coupled dictionary learning considers the problem of learning jointly two dictionary matrices, $\mathbf{D}_X$,$\mathbf{D}_Y$, representing the coupled feature spaces X and Y, such that both representations share approximately the same sparse coding. In our formulation, we consider a set composed of correspondent high and low spectral resolution hypercubes. We assume that these scenes are realized by the same statistical process under different spectral resolution conditions, and as such, they share approximately the same sparse code with respect to their corresponding dictionaries, $\mathbf{D}_h$ and $\mathbf{D}_\ell$. A straightforward strategy to create these dictionaries is to randomly sample multiple correspondent "hyper-pixels" and use this random selection as the sparsifying dictionary. However, such a strategy is not able to guarantee that the same sparse code can be utilized among the two different representations. In order to overcome this limitation, we propose learning a compact dictionary from such pairs of high and low-spectral resolution data-cubes.

Consequently, the joint dictionary learning problem is formulated as:

$$\min_{\mathbf{D}_j,\mathbf{X}} ||\mathbf{P}-\mathbf{D}_j\mathbf{X}||_2^2+\lambda||\mathbf{X}||_1, \text{ s.t } ||\mathbf{D}_j(:,i)||_2^2 \leq 1 \quad (4)$$

where $\mathbf{D}_j = \begin{bmatrix}\mathbf{D}_h\\ \mathbf{D}_\ell\end{bmatrix} \in \mathbb{R}^{(M+N)\times L}$, $M+N$ denotes the concatenated number of spectral bands for both high and low-spectrum scenarios, L is the number of dictionary atoms, and $\mathbf{P} = \begin{bmatrix}\mathbf{S}_h\\ \mathbf{S}_\ell\end{bmatrix}$ corresponds to the set of "hyper-pixels" extracted from the training pairs of high and low-spectral resolution hyperspectral images.

The problem in Eq. 4 can be efficiently solved via the state-of-the-art K-SVD dictionary learning algorithm [12], [13], alternating between two stages: the sparse coding and the dictionary update. Fig. 1 presents the proposed system's block diagram, where we summarize the individual steps for our scheme in recovering the full spectrum from a limited number of acquired spectral bands.

V. Experimental Results

This section demonstrates the performance of the proposed sparse coding scheme when applied to the spectral super-resolution of satellite hyperspectral imagery from perspectives of both the quality and the fidelity of the high spectral resolution 3D data-cubes. To evaluate the effectiveness of the proposed technique, we conducted experiments on hyperspectral data acquired by NASA's EO-1 mission's Hyperion hyperspectral instrument. Due to its high spectral coverage, Hyperion scenes have been widely utilized for multiple remote sensing applications, including classification and spectral unmixing purposes among others. Specifically, Hyperion instrument resolves 220 spectral bands covering the range from 0.4 to 2.5 μm. However, in our simulations we considered only 39 spectral bands from the visible and near-infrared (VNIR) region, with an average wavelength between $437-833$ nm (Bands:9-48). In our simulations, band 9 corresponds to our first spectral band, while band 48 stands for the 39th spectral band. Concerning the testing phase, we utilized several hyperspectral scenes depicting variant regions of Hawaii island, acquired on August 30, 2015. The ground truth 3D data-cubes are down-sampled by a factor of 2,3 and 4 to generate the low and high spectral resolution pairs for both training and evaluation.

A. *Evaluation Metrics*

In order to assess the quality of the reconstructed 3D data-cubes, we employed the Peak Signal to Noise Ratio (PSNR) [16] metric formulated as:

$$PSNR = 10\log_{10}[L_{max}^2/MSE(x,y,\lambda)],$$

where L is the maximum pixel value of the scene, λ denotes the spectral dimension, and MSE stands for the mean square error, defined as:

$$\text{MSE}(x,y,\lambda) = \frac{\sum_{x,y,\lambda}\left[\mathbf{S}_{h_{(x,y,\lambda)}} - \mathbf{S}_{\ell_{(x,y,\lambda)}}\right]^2}{n_x, n_y, \lambda}, \quad (5)$$

where x and y denote the spatial dimensions of the input and the synthesized images $\mathbf{S}_\ell$ and $\mathbf{S}_h$. Additionally, each estimated spectral band is compared against the corresponding ground truth spectral band in terms of the *Structural Similarity Index Metric* [25], a psychophysically modeled error metric defined as:

$$\text{SSIM}(x,y) = \frac{(2\mu_x\mu_y + c1)\cdot(2\sigma_{xy}+c_2)}{(\mu_x^2+\mu_y^2+c_1)\cdot(\sigma_x^2+\sigma_y^2+c_2)}, \quad (6)$$

where μ and σ stand for the mean value and the standard deviation, respectively. The performance of the proposed approach, is compared against the results obtained through cubic interpolation among the spectral bands.

B. *Remote Sensing Data Recovery*

Concerning the dictionary training phase, we utilized multiple hyperspectral scenes acquired by the Hyperion sensor. For the high spectral resolution dictionary, the number of bands is set to 39, while for the low spectral resolution dictionary the down-sampling factor was set to 2, 3 and 4, resulting in 20, 13 and 10 input spectral

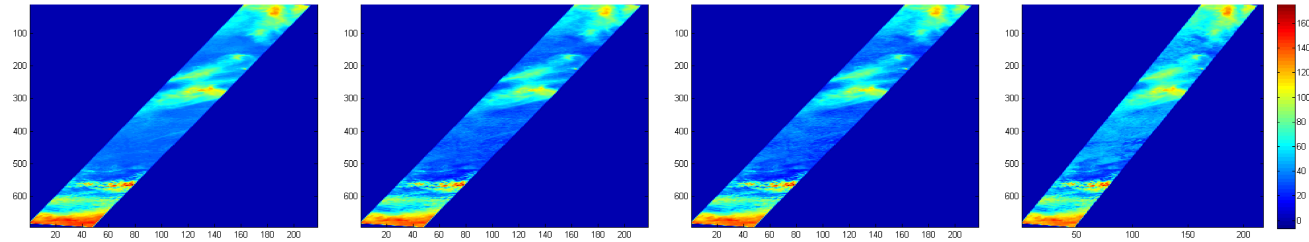

(a) 13th Band (ground truth) (b) 28th Band (ground truth) (c) 35th Band (ground truth) (d) 47th Band (ground truth)

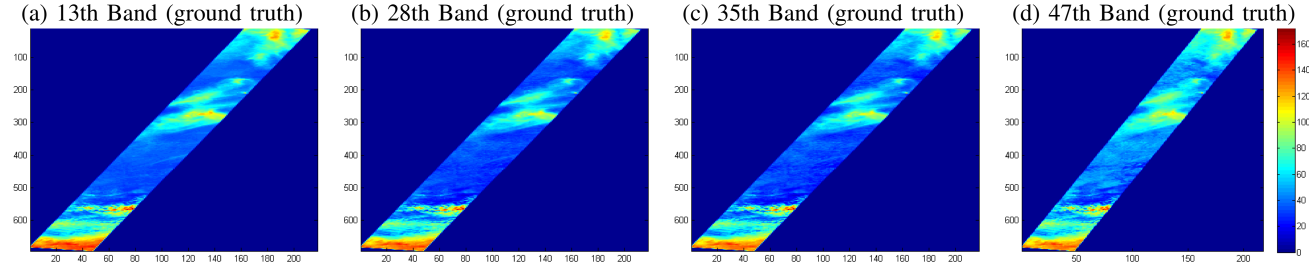

(e) (x2) 13th recovered (SSIM 0.9942) (f) (x2) 28th recovered (SSIM 0.9899) (g) (x2) 35th recovered (SSIM 0.9960) (h) (x2) 47th recovered (SSIM 0.9879)

Fig. 2: Hyperion spectral bands reconstruction: (Top row) Original spectral bands (13th, 28th, 35th, 47th). (Bottom row) Proposed system's reconstructed spectral bands. We observe that under real life conditions, the proposed scheme produces significant quality improvement, operating in satellite hyperspectral imagery. The full spectrum is composed of 39 bands in the VNIR region, while the sub-sampling factor is set to 2.

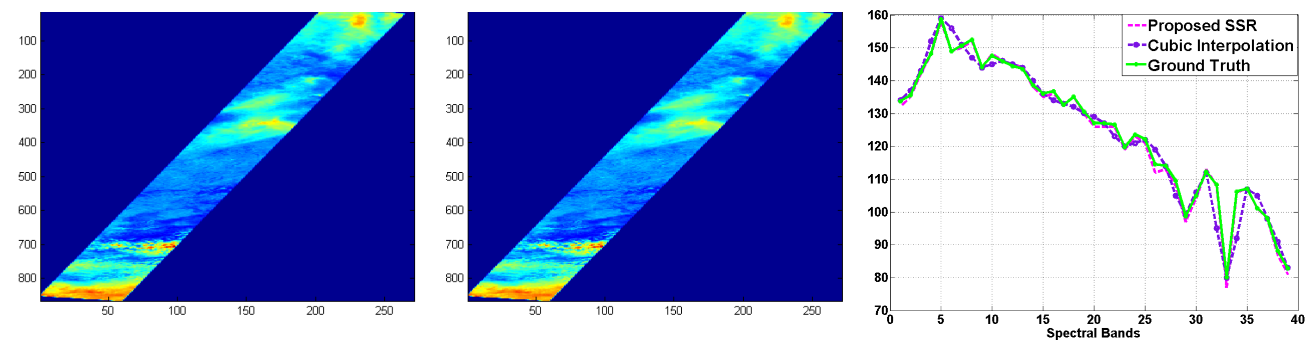

(a) (x2) Cubic Interpolation 47th Band, PSNR: 46.57 dB (b) (x2) K - SVD SSR Recovered 47th Band, PSNR: **55.04** dB (c) Spectral Signatures of the calibrated spectral bands: Ground truth 47th band corresponds to our 39th spectral band

Fig. 3: Hawaii scene II: Reconstruction of the full hypercube. In this simulation we investigate the performance of the proposed system vs. the Cubic interpolation when is applied on the full hypercube of Hawaii test scene II. We recover 39 from 20 input spectral bands and simultaneously provide the spectral signatures of the comparable techniques. The proposed system's spectral signature depicts high similarity with the ground truth's hypercube spectral signature. Additionally, in terms of PSNR error, the proposed technique outperforms in comparison with the Cubic interpolation.

bands,respectively. Consequently, we learned three dictionaries composed of 512 atoms, from 100K randomly sampled "hyper-pixels", each one corresponding to the different sub-sampling factors. The number of selected dictionary atoms balances between a proper representation of the high spectral resolution "hyper-cubes" and a small run-time.

Fig. 2 demonstrates several recovered spectral bands from the Hyperion sensor, along with their ground truth results. In this simulation the sub-sampling factor is set to 2, and we recovered the full-spectrum composed of 39 spectral bands, from only 20 spectral observations. As we may observe, the recovered spectral bands depict high similarity with the ground truth spectral slices, both visually and quantitatively in terms of the similarity index. In fig. 3 we compare the performance of our proposed scheme with the state-of-the-art framework of Cubic interpolation. Additionally, we observe that

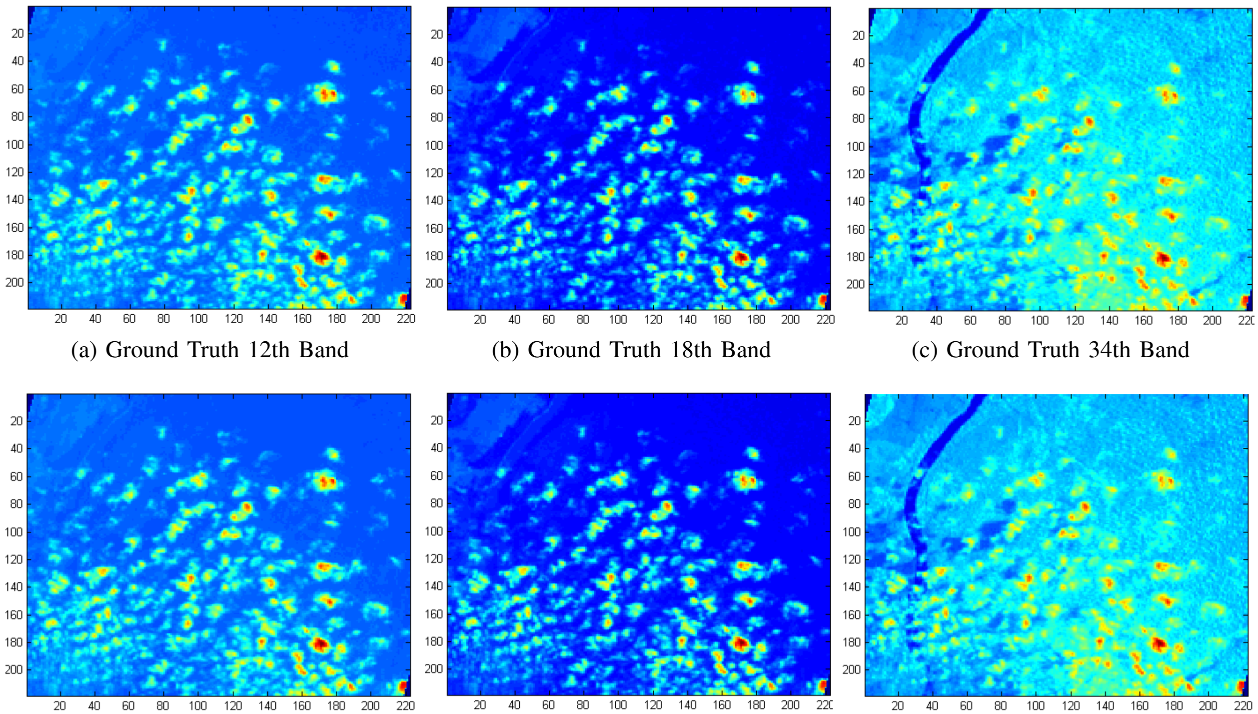

(a) Ground Truth 12th Band (b) Ground Truth 18th Band (c) Ground Truth 34th Band

(d) (x2) Proposed, recovered 12th band (SSIM: 0.9942) (e) (x2) Proposed, recovered 18th band (SSIM: 0.9975) (f) (x2) Proposed, recovered 34th band (SSIM: 0.9977)

Fig. 4: **Hawaii Scene I**: (Top row) Original spectral bands (12th, 18th, 34th). (Bottom row) Proposed system's reconstructed spectral bands. We observe that under real life conditions, the proposed scheme produces significant quality improvement, operating in satellite hyperspectral imagery. The full spectrum is composed of 39 bands in the VNIR region, while the sub-sampling factor is set to 2.

the proposed scheme's spectral signature depicts high similarity with the spectral signature of the ground truth 3D data-cube, highlighting the high quality of our reconstruction. Finally, the PSNR error for the whole 3D cube reconstruction is $\mathbf{55.04}$ dB, while the Cubic's interpolation PSNR is 46.57 dB.

In fig. 4 we illustrate another simulation applied on a specific 203×204 region of the Hawaii I, 3D data-cube. As we may observe the proposed spectral resolution enhancement scheme reveals significant information details among the different spectral bands, that preserve accurate similarity with the ground truth spectral bands, both visually and quantitatively in terms of the SSIM metric. The comparison of Hawaii I scene with the state-of-the-art approach of Cubic interpolation is depicted in fig. 5, where we observe the high quality reconstruction of the proposed scheme when it is applied on the 47th spectral band. Additionally, the proposed system's spectral signature matches accurately with the ground truth's hypercube. Finally, fig. 6 depicts the reconstruction perfomance of the comparable methods applied on Hawaii scene II. The magnification factor in this case is set to 3. In contrast to the Cubic's Interpolation scheme that presents a slight blurring effect, the proposed system preserves accurate similarity with the ground truth hypercube both quantitatively and qualitatively.

VI. CONCLUSIONS

The proposed inverse spectral resolution enhancement problem recovers high spectral information, capitalizing on the sparse representations framework as prior-knowledge, effectively encoding the relationships between high and low spectral representations. Additionally, the proposed scheme can be extended to handle large ranges of low-to-high resolution enhancements by efficient modifications of the joint dictionary learning process, as well as offering the capability of addressing additional sources of HSI image degradation such as blurring and noise.

ACKNOWLEDGMENT

This work was funded by the PHySIS project, contract no. 640174, and by the DEDALE project no.

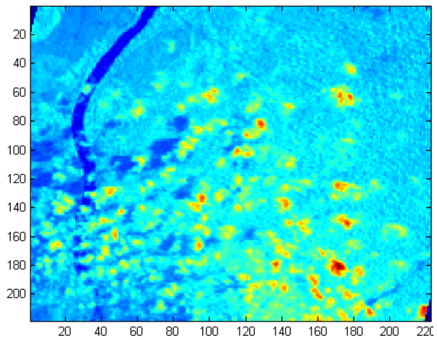

(a) (x4) Ground Truth 47th Band

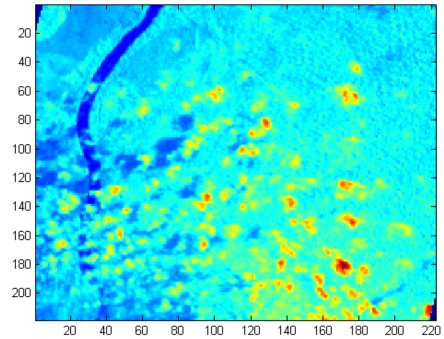

(b) (x4) Cubic Interpolation 47th Band, PSNR: 28.03 dB

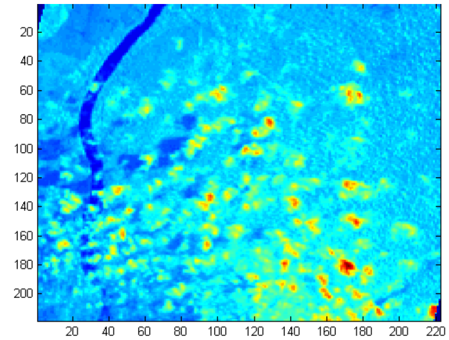

(c) (x4) K-SVD - SSR 47th Band, PSNR: **35.07** dB

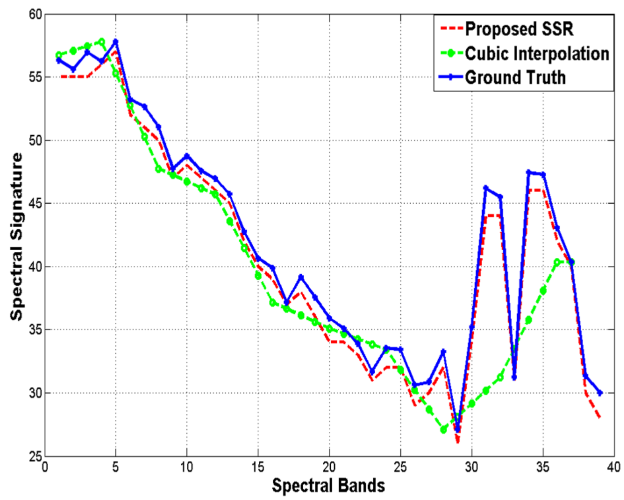

(d) Spectral Signatures of the calibrated spectral bands: Ground truth 47th band corresponds to our 39th spectral band

Fig. 5: **Hawaii scene I**: In this simulation we investigate the perfomance of the proposed system vs. the Cubic Interpolation technique. The sub-sampling factor is set to 4. (Top row:) Comparable techniques illustrating the 47th spectral band. (Bottom row:) Spectral signatures of the comparable methods. As we may observe, the proposed technique preserves an accurate spectral signature with the ground truth 3D data-cube.

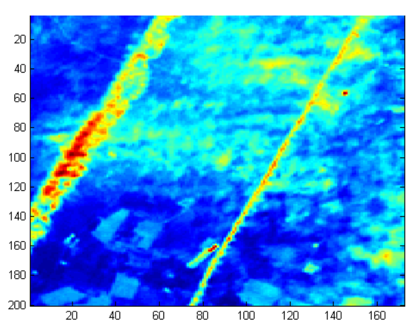

(a) (x3) Ground Truth 11th Band

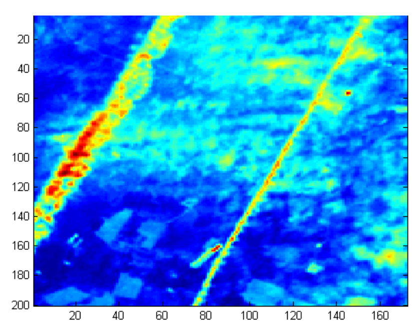

(b) (x3) Cubic Interpolation 11th Band, PSNR: 20.53 dB

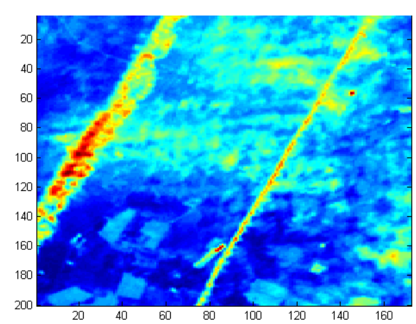

(c) (x3) K-SVD - SSR 11th Band, PSNR: **29** dB

Fig. 6: **Hawaii scene II**: Comparison with the state-of-the-art. In this simulation we set the sub-sampling factor to 3. We observe that the proposed system depicts a smoother visual result in comparison with the Cubic's interpolation result. Additionally, in terms of quantitative evaluation for the reconstruction of the 3D data-cube the proposed system achieves higher PSNR error compared to the Cubic's interpolation scheme.

TABLE I: Hyperion's hyperspectral scenes: Quantitative performance evaluation of the proposed SSR- K-SVD scheme with the state-of-the-art in terms of PSNR error (dB) with magnification factors of 2,3 and 4.

Image	Scale	Cubic	Proposed
Hawaii scene I	2	40.58	**47.89**
Hawaii scene II	2	33.18	**44.32**
Hawaii scene III	2	46.13	**48.50**
average	2	39.96	46.90
Image	Scale	Cubic	Proposed
Hawaii scene I	3	26.55	**31.63**
Hawaii scene II	3	20.53	**29.75**
Hawaii scene III	3	22.39	**36.21**
average	3	23.15	**32.53**
Image	Scale	Cubic	Proposed
Hawaii scene I	4	28.03	**35.07**
Hawaii scene II	4	20.71	**29.61**
Hawaii scene III	4	22.23	**24.33**
average	4	23.65	**29.67**

665044 within the H2020 Framework Program of the European Commission.

REFERENCES

[1] M. Elad: Sparse and Redundant Representations: From Theory to Applications in Signal and Image Processing. Springer (2010).

[2] K. Fotiadou, G. Tsagkatakis, P. Tsakalides. Spectral Resolution Enhancement of Hyperspectral Images via Sparse Representations. (In Proceedings) Proc. Computational Imaging, IS&T Int. Symposium on Electronic Imaging. 2016.

[3] B.Geelen, T.Nicolaas, L.Andy. A compact snapshot multispectral imager with a monolithically integrated per-pixel filter mosaic. In: Spie Moems-Mems. International Society for Optics and Photonics, 2014.

[4] B.Geelen, et al. : A tiny VIS-NIR snapshot multispectral camera.InL SPIE OPTO. International Society for Optics and Photonics, 2015.

[5] Alparone, L., Wald, L., Chanussot, J., Thomas, C., Gamba, P., Bruce, L.: Comparison of pansharpening algorithms: Outcome of the 2006 GRS-S data-fusion contest. IEEE Trans. Geoscience. Remote Sensing. 45(10) (Oct 2007) 3012-3021

[6] Wang, Suyu, Bo Wang, and Zongxiang Zhang: Spatial resolution enhancement of hyperspectral images based on redundant dictionaries. Journal of Applied Remote Sensing 9.1 (2015): 097492-097492.

[7] Zhao, Yongqiang, et al: Coupled hyperspectral super-resolution and unmixing. In Geoscience and Remote Sensing Symposium (IGARSS), 2014 IEEE International. IEEE, 2014.

[8] A. Erturk, M. K. Gullu, D. Cesmeci, D. Gercek, & S. Erturk (2014). Spatial resolution enhancement of hyperspectral images using unmixing and binary particle swarm optimization. Geoscience and Remote Sensing Letters, IEEE, 11(12), 2100-2104.

[9] G. Tsagkatakis, M. Jayapala, B. Geelen, P. Tsakalides. Non-negative Matrix Completion for the Enhancement of Snapshot Mosaic Multispectral Imagery (In Proceedings) Proc. Image Sensors and Imaging Systems, IS&T Int. Symposium on Electronic Imaging, pp. 1?1, 2016.

[10] H. F., A. Parada, and H. Arguello: Spectral resolution enhancement of hyperspectral imagery by a multiple-aperture compressive optical imaging system. In: Ingeniera e Investigacion 34.3 (2014): 50-55.

[11] Charles, A. S., C. J. Rozell, and N. B. Tufillaro: Sparsity based spectral super-resolution and applications to ocean water color. In: IGARSS 2014. Technical Abstract (2014).

[12] M. Aharon, M. Elad, A. Bruckstein, Y. Katz: K-SVD: An Algorithm for Designing of Over-complete Dictionaries for Sparse Representations. In: IEEE Trans. on Signal Processing, (Volume: 54, Issue: 11), pp. 4311-4322, (Nov.2006).

[13] M. Aharon, M. Elad, and A. M. Bruckstein. K-svd and its non-negative variant for dictionary design. In Optics & Photonics 2005, pages 591411?591411. International Society for Optics and Photonics, 2005

[14] Minghelli-Roman, A., Polidori, L., Mathieu-Blanc, S., Loubersac, L., Cauneau, F.:Spatial resolution improvement by merging MERIS-ETM images for coastal water monitoring. IEEE Geosci. Remote Sens. Lett. 3(2) (April 2006) 227-231

[15] N. Akhtar, F. Shafait, and A. Mian: Sparse spatio-spectral representation for hyperspectral image super-resolution. In ECCV, pages 63 ? 78, Sept. 2014.

[16] Singh, Arvind Kumar, et al: Quality metrics evaluation of hyperspectral images.In: ISPRS-International Archives of the Photogrammetry, Remote Sensing and Spatial Information Sciences 1 (2014): 1221-1226.

[17] A. Lambrechts, et al.: A CMOS-compatible, integrated approach to hyper-and multispectral imaging. In: Electron Devices Meeting (IEDM), 2014 IEEE International. IEEE, 2014.

[18] J. Yang, J. Wright, T. Huang, Y. Ma: Image Super-Resolution via Sparse Representations, In: Image Processing, IEEE Trans. on (Vol.19, Issue: 11), pp. 2861-2873. (Nov. 2010).

[19] J. Tropp, A. C. Gilbert, et al. Signal recovery from random measurements via orthogonal matching pursuit. in: IEEE Trans. on Information Theory, 53(12):4655?4666, 2007.

[20] R. Tibshirani. Regression shrinkage and selection via the lasso. Journal of the Royal Statistical Society. Serie. B (Methodological), pages 267?288, 1996.

[21] Fotiadou, Konstantina, Grigorios Tsagkatakis, and Panagiotis Tsakalides: Low Light Image Enhancement via Sparse Representations. In: Image Analysis and Recognition. Springer International Publishing, 2014. 84-93.

[22] G. Tsagkatakis, and P. Tsakalides: Compressed hyperspectral sensing. In: IS&T/SPIE Electronic Imaging. International Society for Optics and Photonics, 2015.

[23] G. Tsagkatakis, and P. Tsakalides: Recovery of Quantized Compressed Sensing Measurements. In: Proc. 2015 IS&T/SPIE Electronic Imaging Conference, Computational Imaging XIII, San Francisco, CA, February 8-12, 2015.

[24] Karalas, Konstantinos, et al: Deep learning for multi-label land cover classification. In: SPIE Remote Sensing. International Society for Optics and Photonics, 2015.

[25] Z. Wang, A. C. Bovik, H. R. Sheikh, and E. P. Simoncelli. Image quality assessment: From error visibility to structural similarity. Trans. Img. Proc., 13(4):600?612, Apr. 2004

[26] https://eo1.usgs.gov/sensors/hyperion